Article

Journal of Tissue Engineering
Volume 5: 1–10

DOI: 10.1177/2041731414536573
tej.sagepub.com
SAGE

Cefazolin-loaded mesoporous silicon microparticles show sustained bactericidal effect against *Staphylococcus aureus*

Iman K Yazdi[1,2], Matthew B Murphy[1], Christopher Loo[1], Xuewu Liu[1], Mauro Ferrari[1], Bradley K Weiner[1,3], and Ennio Tasciotti[1]

Abstract

Cefazolin is an antibiotic frequently used in preoperative prophylaxis of orthopedic surgery and to fight secondary infections post-operatively. Although its systemic delivery in a bulk or bolus dose is usually effective, the local and controlled release can increase its effectiveness by lowering dosages, minimizing total drug exposure, abating the development of antibiotic resistance and avoiding the cytotoxic effect. A delivery system based on mesoporous silicon microparticles was developed that is capable of efficiently loading and continuously releasing cefazolin over several days. The in vitro release kinetics from mesoporous silicon microparticles with three different nanopore sizes was evaluated, and minimal inhibitory concentration of cefazolin necessary to eliminate a culture of *Staphylococcus aureus* was identified to be 250 μg/mL. A milder toxicity toward mesenchymal stem cells was observed from mesoporous silicon microparticles over a 7-day period. Medium pore size-loaded mesoporous silicon microparticles exhibited long-lasting bactericidal properties in a zone inhibition assay while they were able to kill all the bacteria growing in suspension cultures within 24 h. This study demonstrates that the sustained release of cefazolin from mesoporous silicon microparticles provides immediate and long-term control over bacterial growth both in suspension and adhesion while causing minimal toxicity to a population of mesenchymal stem cell. Mesoporous silicon microparticles offer significant advantageous properties for drug delivery applications in tissue engineering as it favorably extends drug bioavailability and stability, while reducing concomitant cytotoxicity to the surrounding tissues.

Keywords

Antibiotics, controlled release, drug delivery, microparticles, mesoporous silicon

Received: 12 February 2014; accepted: 28 April 2014

Introduction

Orthopedic surgeries represent a substantial portion of total medical treatments in the United States with over 25.8 million procedures or consultations related to the back or spine, 14.5 million for knee problems, and 9.7 million for shoulder injuries.[1] Even with modern sterilization and aseptic surgical techniques, orthopedic surgery is still associated with infectious complications, especially in the setting of intervention after traumatic injuries. Approximately 1–3 out of every 100 patients who have surgery develop infection, representing one-fourth of all nosocomial infections.[2] Treatment of implant-related infections, on the other hand, involves long-term systemic administration of antibiotics and multiple operations to remove hardware and locally decontaminate the surgical field. Serious problems can arise from this approach, including a failure to produce therapeutic tissue concentrations of the antibiotics secondary to poor tissue perfusion,

[1]Department of Nanomedicine, Houston Methodist Research Institute, Houston, TX, USA
[2]Department of Biomedical Engineering, University of Houston, Houston, TX, USA
[3]Department of Orthopedic Surgery, Houston Methodist Hospital, Houston, TX, USA

Corresponding author:
Ennio Tasciotti, Department of Nanomedicine, Houston Methodist Research Institute, 6670 Bertner Avenue, Houston, TX 77030, USA.
Email: etasciotti@houstonmethodist.org

selection of highly resistant bacteria through repeated low-dose exposure, and the multiple complications associated with the subsequent operations to repair the problem.[3]

According to the guide for elimination of orthopedic surgical site infections published by the Association for Professionals in Infection Control and Epidemiology (APIC), *Staphylococcus aureus* is considered as one of the major Gram-positive microorganisms associated with surgical site infections, possesses a high degree of virulence due to its ability to produce toxins and develop resistance to many classes of antibiotics, and is accounted for 48.6%.[4] Antimicrobial agents are decided according to the type of microorganism based on the clinical practice guidelines for post-surgical infections. Cefazolin serves as the standard of care and first drug of choice according to the current practice in antimicrobial prophylaxis.[5] It has been the most widely used agent with confirmed efficacy against *S. aureus* as well as widely common organisms encountered in surgery such as *Escherichia coli* and various strains of *Streptococci, Proteus mirabilis*, and *Klebsiella* species.[6]

Ideally, an antibiotic delivery system should provide sustained and controlled release to nearby tissues, eliminating the need for systemic infusions or repeated injections of the drug.[7–9] Localized release allows for total dose reduction and minimizes systemic toxicity and resistance, and various biodegradable and bioresorbable carriers of antibiotics for the treatment and prevention of prosthetic infections have been studied.[10–12] Therefore, many materials have been introduced and chemically modified to maintain extended-release properties in the past decade.[13] Simultaneously, with the development of new polymers[14–17] and inorganic porous matrices,[18–23] nanotechnology has increasingly influenced the field.[24,25] One of the widely used techniques to deliver antibiotics locally to a wound site is through the introduction of polymethylmethacrylate (PMMA) beads or poly(lactic-co-glycolic acid) (PLGA) particles loaded with antibiotic. Although effective for treating most infections, these polymeric materials are not always fully bioresorbable and their acidic degradation byproducts locally irritate surrounding tissues, create acute inflammation, and may elicit an immune response thus hampering tissue healing.[26,27]

Porous silicon-based biomaterials with nanoscale features[28–33] are appealing for this purpose, as their release and degradation kinetics[34] are tunable as a function of porosity and pore size.[35–37] Mesoporous silicon microparticles (MPS) can enhance drug availability and distribution over time similar to PLGA particles as they degrade to control the payload release kinetics with a negligible inflammatory tissue response and no toxic side effects in vivo.[38–40]

Previously, MPS have been employed for the targeted or controlled delivery of ibuprofen, griseofulvin, ranitidine, furosemide, antipyrine, daunorubicin, Q-dots, ethionamide, peptides, RNA interference, and imaging agents.[41–48] In this work, we have shown the release kinetics of cefazolin with three different nanopore sizes of MPS, bactericidal activity of them on *S. aureus*, as one of the most prevalent bacteria strains associated with post-operative infections,[49–51] and also cytotoxicity effects of antibiotic-loaded MPS toward mesenchymal stem cells (MSCs) to ensure this technology would be conducive for wound repair and tissue regeneration.[33,52]

Materials and methods

Preparation and characterization of porous silicon microparticles

Microparticles of three different pore sizes were generated and characterized for this study: small pore (SP), medium pore (MP), and large pore (LP) MPS with mean pore diameters of 3, 6, and 10 nm, respectively. All microparticles had a mean diameter of 3.2 ± 0.2 μm. MPS were designed and fabricated in the Microelectronics Research Center at The University of Texas at Austin as previously reported.[37,53,54] Briefly, heavily doped p++ type (100) silicon wafers (Silicon Quest, Inc., San Jose, CA, USA) were used as the base for the deposition of a 200-nm layer of silicon nitride using low-pressure chemical vapor deposition followed by standard photolithography with an EVG 620 contact aligner. To produce a highly porous layer, current density of 320 mA/cm^2 was applied for 6 s in a 49% mixture of hydrofluoric acid (HF) in ethanol (2:5 (v/v)).[37] The particle surface was further oxidized by H_2O_2, and then the suspension was heated to 100°C–110°C for 4 h, washed with deionized water, and resuspended in isopropyl alcohol (IPA). The morphology of MPS was examined in detail by scanning electron microscopy (SEM) and transmission electron microscopy (TEM).

Microparticle size and charge characterization

MPS volume, size, count, and charge were obtained using a Multisizer™ 4 Coulter Counter (Beckman Coulter, Inc., Brea, CA, USA) and Zetasizer Nano ZS (Malvern Instruments, Inc., Westborough, MA, USA). Before the analysis, the samples were dispersed in a balanced electrolyte solution and sonicated for 10 s for sufficient dispersion. The zeta-potential of the microparticles was analyzed by a Zetasizer Nano ZS.[55] For all analyses, 2 μL particle suspension containing at least 1×10^5 particles to achieve a stable zeta-value evaluation was injected into a sample cell countering field with phosphate buffer (1.4 mL, pH 7.2). The cell was sonicated for 2 min, and then an electrode probe was placed into the cell. Measurements were conducted at room temperature (23°C) in triplicate runs.

Antibiotic loading

A volume of 10^7 MPS/mL was combined with a concentrated antibiotic solution (cefazolin sodium, 5 mg/mL in phosphate buffered saline (PBS); Sigma–Aldrich, St. Louis, MO, USA) at room temperature. The MPS and loading solution were sealed in a centrifuge tube, which was gently stirred during the loading process for 1 h. After loading, the MPS were separated by centrifugation from the solution, rinsed twice with PBS to wash off any drug substance from their surface, and lyophilized overnight. The loading efficiency was determined by high-performance liquid chromatography (HPLC) and confirmed by the cumulative release of cefazolin from the particles.

Analytical method to determine cefazolin concentration

A mobile buffer solution composed of 20% methanol, 10% acetonitrile, and 70% monobasic phosphate buffer was passed through an Agilent ZORBAX SB-C18 column (4.6 mm inside diameter (ID) × 250 mm length).[56] The buffer was passed through the column at a rate of 0.5 mL/min, and the absorbance of cefazolin in solution was measured at a wavelength of 270 nm on a Hitachi L-2455 Diode Array Detector. The retention time for cefazolin was 2.5–3.0 min. Injection volumes were 20 μL for all samples. Standard curves were created with serial dilutions of cefazolin in PBS, so that linear regression could be used to determine sample concentrations based on peak height and retention time area. All HPLC measurements were performed at room temperature.

In vitro drug release

Individual batches of cefazolin-loaded MPS (10^7 particles) were incubated in 1 mL of fresh PBS solution in a humidified 95% air/5% v/v CO_2 incubator at 37°C with gentle shaking (100 rev/min). The release solution was collected and replaced by fresh PBS at every time points. Drug concentration was determined by measuring the collected solution with HPLC and ultraviolet (UV)–visible (Vis) spectroscopy. Three samples were measured for each time point and the results were reported as average values ± standard deviation (SD). Samples were collected until no additional cefazolin was released (5 days).

Antibacterial assessment

Minimum inhibitory concentration assay. The toxicity of cefazolin sodium to *S. aureus* ATCC 29213 was investigated by adding 0, 50, 100, 250, and 500 μg/mL to 1 mL of 10^6 colony-forming unit (CFU)/mL bacterial suspension. Cells were counted at 3, 6, 12, 24, 48, and 72 h, with triplicate samples at each time point using conventional plate count method.

Determination of the zones of inhibitory concentration. A measure of 1.5 mL from a 10^6 CFU/mL Luria Bertani Broth (LB) suspension was added to the 37°C pre-warmed nutrient agar medium (BD Falcon 100 × 15 mm style) plates and incubated at 37°C for 24 h. Cefazolin-loaded MPS (250 μg in 10^7 SP or MP particles in 50 μL PBS) were deposited at four equidistant locations on the agar plates and left at room temperature for 30 min before incubation at 37°C. The diameters of inhibition zones were measured for days 1, 2, 3, 7, and 21 and expressed as mean ± SD. The corresponding positive (with equivalent concentrations of cefazolin to loaded particles in PBS) and negative (using unloaded microparticles without antibiotic) controls were prepared and tested.

Antimicrobial activity assay. *S. aureus* bacteria were suspended in 2.5 mL of sterile-rich LB broth medium. The suspension was standardized using spectrophotometry at a wavelength (λ) of 800 nm to match the transmittance of 90, equivalent to 0.5 McFarland scale (1.5×10^8 CFU/mL). A 2.0 mL volume of the LB broth medium (37°C) was gently poured into a six-well cell culture plate and each well was inoculated with 10^3 CFU/mL of *S. aureus* cells. Antibiotic was added to each well either directly or loaded into MPS. The plates were incubated for 72 h at 37°C and the cells collected and counted at 1, 2, 4, 8, and 24 h. Three replicates were performed for each time point.

Cefazolin and MPS toxicity on rat MSCs

Rat MSCs were isolated from the compact bone of young male Sprague Dawley rats. Tibae and femora were cleaned of periosteum and connective tissue, flushed and washed of marrow, crushed with a mortar and pestle, and enzymatically degraded in a solution of collagenase (3 mg/mL) and dispase (4 mg/mL) in PBS. Liberated mononuclear cells were cultured in media containing 20% fetal bovine serum under hypoxic conditions (5% O_2) to promote colony formation.[57] MSCs from these primary colonies were passaged up to four times prior to toxicity studies.

The cells were seeded in a 24-well plate at a density of 1000 cells/well and allowed to stabilize for 24 h prior to treatment. Rat MSCs were cultured for a period of 7 days, in the above-described experimental conditions as a control, or in complete media supplemented with 0, 50, 100, 250, and 500 μg/mL cefazolin sodium (either direct dose or loaded into 10^7 MPS). Cell proliferation was determined by quantification of double-stranded DNA using the Quant-iT PicoGreen assay (Invitrogen, Carlsbad, CA, USA). Lactate dehydrogenase (LDH) activity assay (Sigma–Aldrich) was used as a determination of cell membrane damage and toxicity. At time points of 1, 5, and 7 days, the culture medium was collected and assayed for LDH cytotoxicity, and the adherent cells were washed

Table 1. Characterization of different types of MPS (small pore, medium pore, and large pore): MPS zeta-potential, particle size (diameter), average pore size, total porosity, and pore volume.

MPS type	Mean zeta-potential (mV) ± SD	Particle size (μm)	Average pore size (nm)	Porosity (%)	Pore volume (fL)
SP	−31.15 ± 1.48	3.2 ± 0.2	3.04 ± 1.08	33	6.34
MP	−27.64 ± 2.73	3.2 ± 0.2	6.02 ± 1.86	47	5.61
LP	−24.73 ± 1.62	3.2 ± 0.2	10.08 ± 3.14	51	4.15

MPS: mesoporous silicon microparticles; SD: standard deviation; SP: small pore; MP: medium pore; LP: large pore.

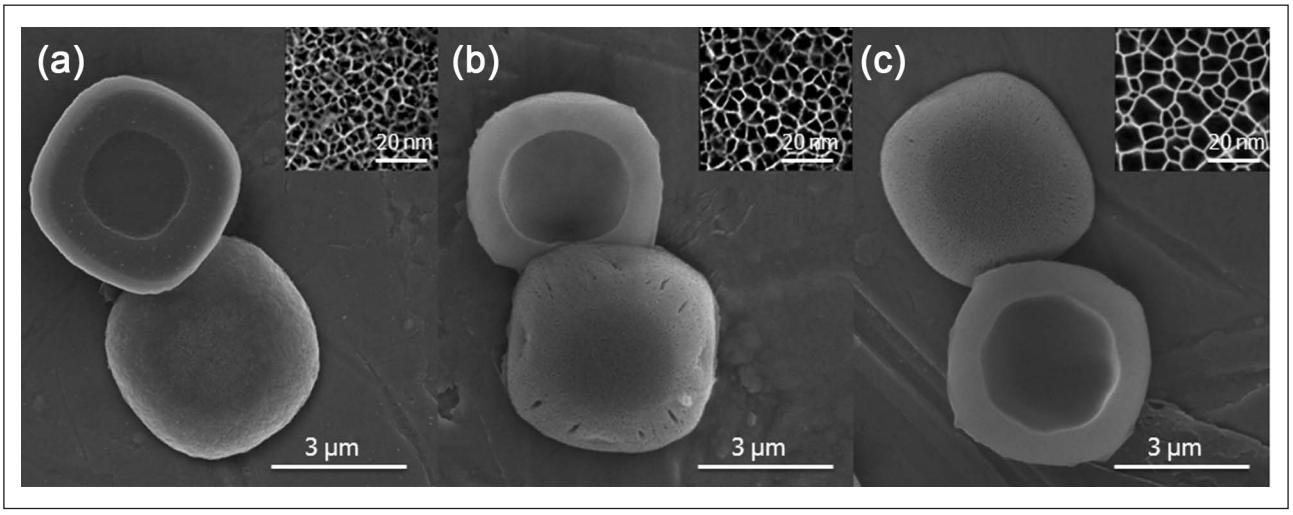

Figure 1. Scanning electron microscopy images of mesoporous silicon microparticles with their relative three different pore sizes: (a) small pore, 3 nm; (b) medium pore, 6 nm; and (c) large pore, 10 nm.

twice with PBS and lysed by addition of 1 mL deionized water and freeze–thawed to −80°C for DNA collection and quantification.

Results and discussion

Characterization of MPS

MPS were fabricated through photolithography and electrochemical etching as previously described.[37] The average diameter of all three MPS types used in this study was evaluated through Multisizer Coulter Counter analysis and their relative surface charge was measured by Nano Zetasizer (Table 1) while the uniformity of the structural properties (aspect ratio, shape, and pore size) was characterized by SEM (Figure 1). Scanning electron micrographs of all different pore size MPS were shown and their pores were presented in more details (Figure 1(a)–(c)). During synthesis and oxidation, the partial surface erosion led to the hydroxylation of MPS creating a net negative charge (Table 1). The direct correlation between MPS pore size and charge was demonstrated through zeta-potential analysis. As the particle pore size increased, the overall porosity increased and the surface area of the particles decreased. Consequently, fewer hydroxyl groups were displayed on MPS surface, causing the net total charge to be less negative (Table 1).

In vitro drug release

The porosification of silicon during electrochemical etching created a large surface area per volume ratio, allowing for the adsorption of high amounts of drug molecules during the loading process. A relationship between the pore diameter and the loading and release profiles of MPS was observed. The parallel-etched pores within the SP microparticles allowed increased drug loading capacity due to their higher surface area than the MP or LP particles. However, total porosity dominates total drug loading mass among these three particle types, as LP possessed the highest total porosity than MP or SP, while SP particles hold the highest surface area among them. The average cefazolin-loaded mass per 10^7 MPS is reported as 275, 392, and 452 μg for SP, MP, and LP microparticles. The amount of antibiotic loaded directly correlated with porosity, pore size, and pore volume as reflected in Figure 2(a). The antibiotic release profiles from cefazolin-loaded MPS obtained over 5 days are shown in Figure 2(b). MPS with larger

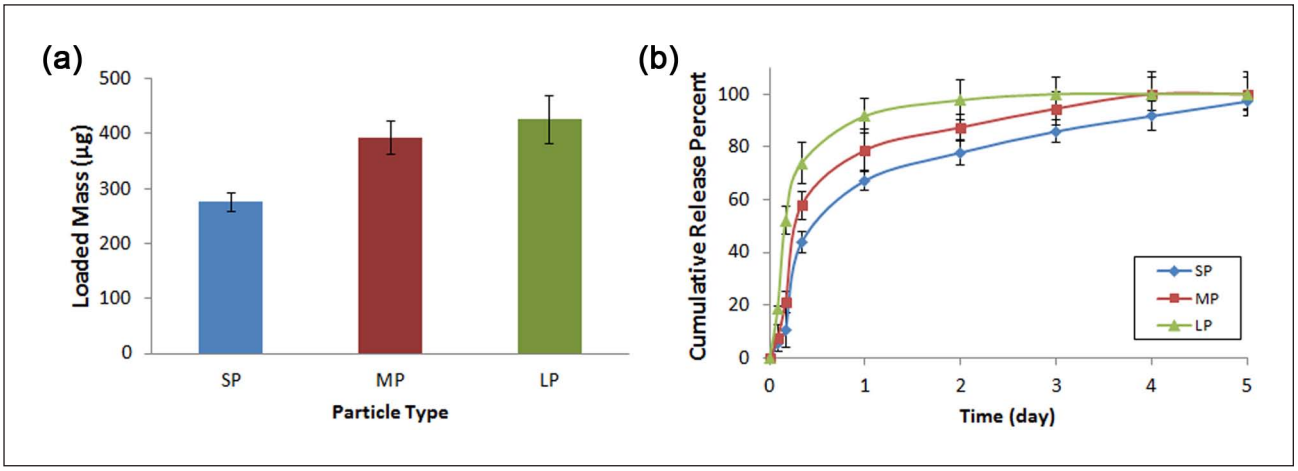

Figure 2. (a) Mass of cefazolin loaded into SP, MP, and LP microparticles (theoretical maximum loading of 5 mg). Higher total porosity of MPS dominates drug loading among these three particle types. (b) The cumulative percentage of released cefazolin as a function of time from SP, MP, and LP particles in vitro over 5 days. The release kinetics delayed with decreasing pore size of MPS, potentially due to the limitations in the diffusion of the drug through pores.
SP: small pore; MP: medium pore; LP: large pore; MPS: mesoporous silicon microparticles.

pores (LP) showed a higher initial burst release of cefazolin.[58] The release delayed with decreasing pore sizes, potentially due to the limitations in the diffusion of the drug through 3 and 6 nm pores (SP and MP). This effect reinforced the notion of the emerging properties of nanostructured materials on drug release kinetics.[59] Complete release was obtained by day 5, at which time the MPS also completely degraded.

Antibacterial activity

The assessment of antibacterial activity of cefazolin-loaded microparticles was tested against *S. aureus*, which is the most common bacterial pathogen seen in osteomyelitis.[60] After the minimum inhibitory concentrations were determined, the antimicrobial activity of the antibiotic-loaded MPS was evaluated by two different techniques: antimicrobial activity and zones of inhibition assay against *S. aureus*.

Minimum inhibitory concentration assay. The antibacterial activity was significantly effective for the three higher cefazolin concentrations. Cefazolin was 90% bactericidal to *S. aureus* ATCC 29213 at concentrations greater than 100 µg/mL. Concentrations of 250 and 500 µg/mL demonstrated more than 98% bacterial elimination within 48 and 24 h, respectively (Figure 3).

Zones of inhibition assay. The bioactivity and potency of the released antibiotic were evaluated using Kirby–Bauer methods determined by creating zones of growth inhibition on agar plates.[61] Disposable agar plates inoculated with the tested *S. aureus* ATCC 29213 at a concentration of 10^6 CFU/mL. SP and MP MPS (10^7 microparticles

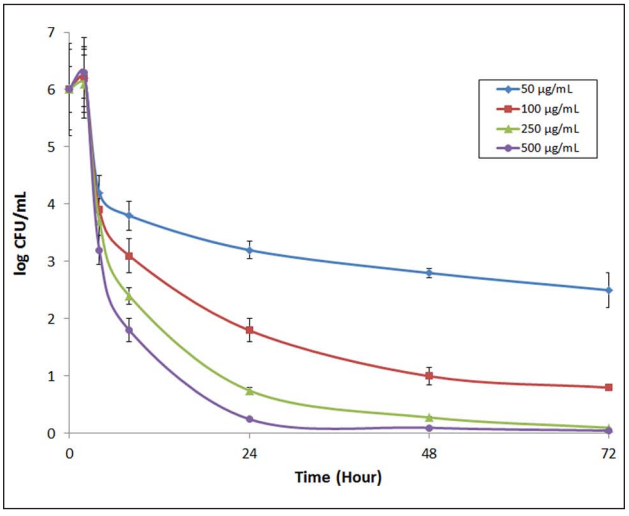

Figure 3. *Staphylococcus aureus* bacteria growth inhibition against 50, 100, 250, and 500 µg/mL of cefazolin sodium over 72 h. Concentrations of 250 and 500 µg/mL demonstrated more than 98% bacterial elimination within 48 and 24 h.
CFU: colony-forming unit.

unloaded or loaded with 250 µg of cefazolin) were selected due to their slower release kinetics for this study and applied to distinct locations of each plate. The diameter of the regions devoid of *S. aureus* growth was measured daily for days 1, 2, 3, 7, and 21. The purpose was to determine the bactericidal effects of the gradual release of cefazolin from MPS. Both particle types showed a significant activity against *S. aureus* by release of cefazolin (Figure 4).

During the first 2 days, the average zones of inhibition obtained with cefazolin-loaded MP treated plates were approximately twice that of SP-treated plates. The

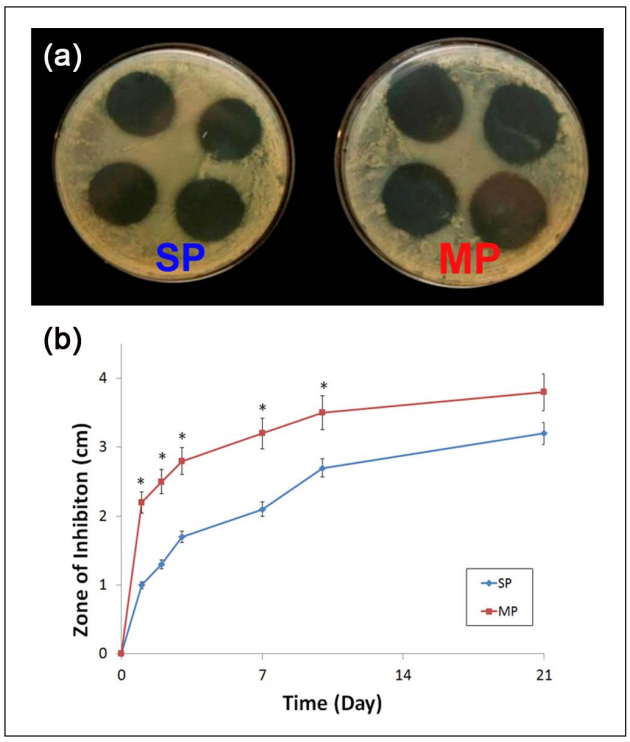

Figure 4. (a) Bacteria inhibition zones surrounding SP and MP cefazolin-loaded MPS (250 µg cefazolin in 107 MPS) at day 21. (b) Zone of inhibition (cm) of SP and MP microparticles over 21 days against *Staphylococcus aureus* from release of cefazolin which indicates a successful long-term elimination and prevention of *S. aureus* growth.
SP: small pore; MP: medium pore; MPS: mesoporous silicon microparticles.

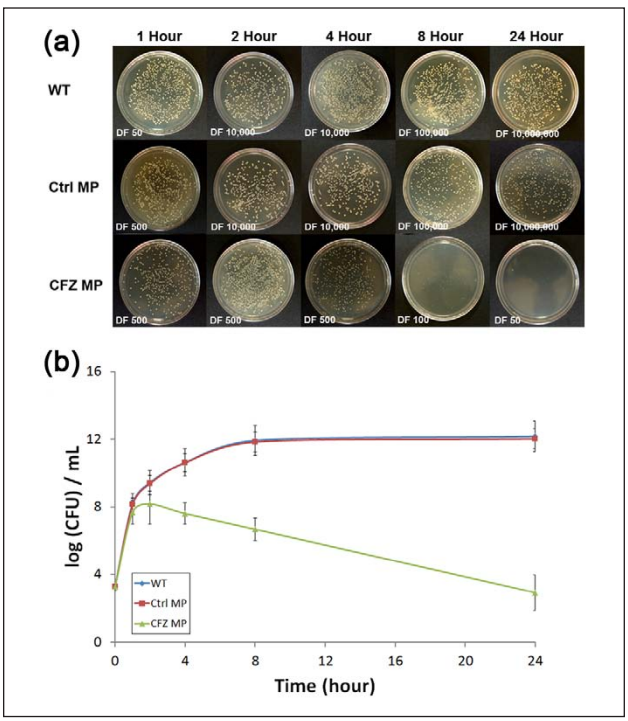

Figure 5. Antimicrobial activity of cefazolin-loaded medium pore MPS against *Staphylococcus aureus*. (a) Bacteria plates were cultured without MPS, with empty or unloaded MPS, or with MPS loaded with 250 µg cefazolin. (b) Bacteria of the WT control and unloaded MPS (Ctrl MP) groups exhibited a growth spike between 4 and 8 h, while the antibiotic particles (CFZ MP) prevented *S. aureus* growth over the course of the 24-h study.
MPS: mesoporous silicon microparticles; WT: wild-type; MP: medium pore; CFU: colony-forming unit.

difference in clear-zone diameter of growth inhibitions of SP and MP was correlated to their release kinetics, respectively, which shows that the zone of inhibition was increased as the amount of loaded cefazolin was increased in MPS. There was no significant difference found in the zone of inhibition between the two particle types once they have completely released their antibiotic payload (from days 10 to 21).

This result successfully indicated a long-term elimination and prevention of *S. aureus* growth in the presence of antibiotic-loaded MPS for up to 21 days. Additionally, unloaded SP and MP MPS control groups did not display any zone of inhibition, meaning the MPS themselves or their degradation byproducts were not responsible for the antimicrobial activity observed.

Antimicrobial activity assay. MP microparticles were selected on the basis of their high loading efficiency and longest inhibitory properties compared to other types of MPS. *S. aureus* was cultured with empty and drug-loaded (250 µg cefazolin) CFZ MP for 24 h. Photographic images of the cultures through the first 24 h are shown in Figure 5(a). Plates with cefazolin-loaded MP microspheres exhibit a significant decrease in the bacteria growth, which correlates with the release of cefazolin within the first 24 h. The wild-type (WT) control exhibited an exponential growth expansion between 4 and 8 h. The number of bacterial colonies (CFU/mL) over the equivalent time range is reported as log(CFU)/mL in Figure 5(b). As determined by the in vitro release study, this growth expansion corresponded with the cumulative release of 40%–50% of the loaded drug by 8 h using the MPS. The controlled release of cefazolin was capable of preventing colony formation throughout the course of the study. There was no inhibitory effect detected for unloaded MP microparticles (Ctrl MP), which indicates that the major bactericidal effect was due to the released antibiotics and not from the microparticle degradation byproducts.

Cefazolin and MPS toxicity on rat MSCs

Rat MSC cell proliferation and cell membrane integrity were evaluated over 7 days to determine the cytotoxic effect of the MPS at various doses of cefazolin. Cell viability at days 1, 5, and 7, normalized against drug-free and MPS-free controls, is reported in Figure 6. Direct

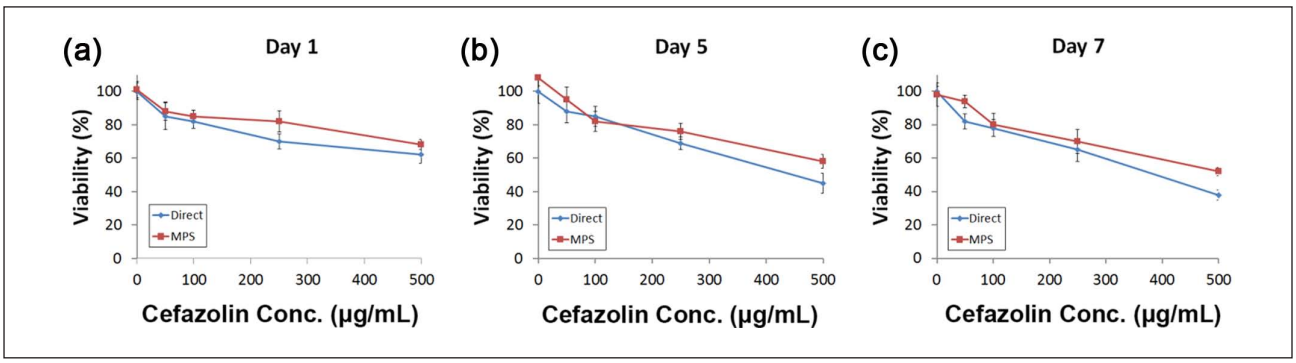

Figure 6. Effects of the presence of different concentrations (50, 100, 250, and 500 µg/mL) of cefazolin (direct dose or release dose from MPS) on the growth of rat MSC showed inhibitory effects on cell growth at much lower concentration on (a) day 1, (b) day 5, and (c) day 7. The controlled release of cefazolin from MPS was able to reduce the cytotoxic effects on MSC compared with direct doses of antibiotic.
MPS: mesoporous silicon microparticles; MSC: mesenchymal stem cell.

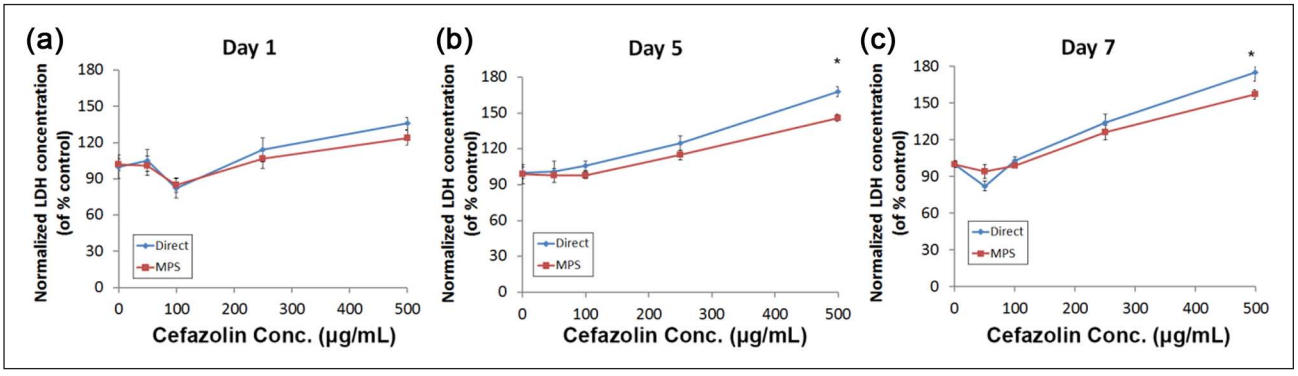

Figure 7. LDH activity in culture media of MSC in the presence of 0, 50, 250, or 500 µg/mL cefazolin either by direct or MPS-sustained delivery at days 1, 5, and 7, normalized against drug-free and MPS-free controls. Sustained release of cefazolin from MPS lessened the harmful effects of direct drug administration at higher concentrations, particularly at days 5 and 7.
LDH: lactate dehydrogenase; MSC: mesenchymal stem cell; MPS: mesoporous silicon microparticles.

administration of the antibiotic had a significant effect on cell viability at 250 and 500 µg/mL. However, the controlled release of cefazolin from MPS caused reduction in the toxic effect of direct exposure of cells to the drug (days 5 and 7). This effect was also observed at 100 µg/mL dosages, although the advantages of MPS were not found statistically significant. Most importantly, the release of 250 µg/mL by MPS, a dose previously was found to exhibit over 98% bactericidal efficacy within 48 h and clearly formation of inhibition zones, was not found to reveal any adverse effects on MSC proliferation and cell membrane integrity, while their direct exposure to a higher concentration of the antibiotic (>250 µg/mL) induced signs of toxicity at all time points. The growth of cells in the presence of antibiotic-loaded MPS was approximately 2%, 13%, 26%, and 18% greater at day 5, and 15%, 7%, 13%, and 18% greater at day 7, than for cells cultured with the direct dose applied of 50, 100, 250, and 500 µg/mL, respectively. Overall the controlled release of cefazolin from MPS was found to reduce the cytotoxic effects on MSC compared with direct doses of antibiotic (Figure 6).

Cell membrane integrity and general cell health were evaluated by LDH release in the culture media at 1, 5, and 7 days after treatment, and the reported results were normalized to cefazolin-free, MPS-free controls in Figure 7. No significant effects were detected for 50 or 100 µg/mL dosages for either the direct treatment or MPS-treated groups. In agreement with MSC viability, dosages of 250 and 500 µg/mL showed enhancement of the LDH activity for both groups at all time points. Likewise, similar levels of LDH production from MSC were observed at 100 µg/mL concentration for both groups. The direct administration of cefazolin exhibited slightly higher LDH activity compared to MPS and the difference was statistically significant at days 5 and 7 for 500 µg/mL ($p < 0.01$). At the three highest dosages used in the study, the sustained release of cefazolin from MPS significantly lessened these cytotoxic effects on MSC compared to the direct administration of cefazolin.

From this investigation, it was found that a local concentration of 250 μg/mL cefazolin was sufficient as an antibacterial prophylactic. Administration of this drug concentration via MPS exhibited no significant effects on MSC cell viability or metabolic integrity compared to controls, while this dosage was found to be toxic to the stromal cells when given as a bulk dose. In contrast to polymeric delivery systems, the MPS are fully degradable and biocompatible and do not generate inflammatory byproducts as the polymeric counterparts.[62–65] It is hypothesized that high local concentrations of antibiotic can diffuse through avascular areas of the surgical or implant site that are inaccessible by systemic intravenous methods, which often can only be delivered in concentrations that may result in toxicity or lead to bacterial antibiotic resistance.

Conclusion

In recent years, the growth of resistant microorganism strains has been accompanied by development of new clinical guidelines and shortage of new formulations. As a result, it is crucial to develop new platforms to maintain the antimicrobial drugs activity while extending their half-lives through new routes of delivery.[66] To overcome these limitations, sophisticated delivery platforms capable of tuning the release of their contents are necessary to fight against drug-resistant bacteria strains such as methicillin-resistant *S. aureus* or *Coagulase-negative Staphylococcus*.[67]

For the past few decades, numerous drug delivery platforms have been developed to enhance the bactericidal properties of antibiotics and meet different clinical needs such as extended shelf-life stability, high biocompatibility, and multifunctional properties.[68–71] In this study, sustained delivery of cefazolin from MPS showed to provide adequate bactericidal properties to efficiently inhibit *S. aureus* growth. The pore size and porosity MPS provide tunable drug release characteristics and their surface area can be modified or encapsulated in order to achieve specific desired therapeutic daily dose for various tissue engineering applications.[72–75] This nanotechnology-based delivery system represents an alternative to the current standard of care and addresses the shortcomings of intravenous antibiotic delivery. The MPS antibiotic delivery system may represent a new platform for the prevention of postoperative infections, for the treatment of biofilm formation on orthopedic implants, and for the medication of traumatic musculoskeletal injuries. Due to its decreased toxicity on stem cells, this system represents a promising alternative to direct administration of the drug, with long-term advantages of the regeneration of the tissues, the healing of the injury, and the overall well-being of the patient.

Acknowledgements

The authors greatly acknowledge the Ernest Cockrell Jr (Distinguished Endowed Chair). The authors thank Dr Dongmei Fan, Dr Enrica De Rosa, Dr Nima Taghipour, Mr Daniel Blashki, and Mr Nitin Warier for their technical supports, and Mr Matthew G. Landry for graphical support.

Declaration of conflicting interests

The authors declare that there is no conflict of interest.

Funding

This study received the financial supports from the Defense Advanced Research Projects Agency (DARPA) through BioNanoScaffolds Fracture Putty program (W911NF-11-1-0266).

References

1. AAOS. Orthopaedic practice in the US 2012 (AAOS census). 2013 http://www.aaos.org/research/orthocensus/census.asp.
2. Hawn MT, Vick CC, Richman J, et al. Surgical site infection prevention: time to move beyond the surgical care improvement program. *Ann Surg* 2011; 254: 494–501.
3. Cantón R and Morosini MI. Emergence and spread of antibiotic resistance following exposure to antibiotics. *FEMS Microbiol Rev* 2011; 35: 977–991.
4. Greene LR. *Guide to the elimination of orthopedic surgical site infections*. APIC, http://www.apic.org/Resource_/EliminationGuideForm/34e03612-d1e6-4214-a76b-e532c6fc3898/File/APIC-Ortho-Guide.pdf (2010).
5. Dale WB and Peter MH. Antimicrobial prophylaxis for surgery: an advisory statement from the National Surgical Infection Prevention Project. *Clin Infect Dis* 2004; 38: 1706–1715.
6. Bratzler DW, Dellinger EP, Olsen KM, et al. Clinical practice guidelines for antimicrobial prophylaxis in surgery. *Am J Health Syst Pharm* 2013; 70: 195–283.
7. Suzuki Y, Tanihara M, Nishimura Y, et al. A new drug delivery system with controlled release of antibiotic only in the presence of infection. *J Biomed Mater Res* 1998; 42: 112–116.
8. Lin S-S, Ueng SW, Liu S-J, et al. Development of a biodegradable antibiotic delivery system. *Clin Orthop Relat Res* 1999; 362: 240–250.
9. Nelson CL. The current status of material used for depot delivery of drugs. *Clin Orthop Relat Res* 2004; 427: 72–78.
10. El-Husseiny M, Patel S, MacFarlane R, et al. Biodegradable antibiotic delivery systems. *J Bone Joint Surg Br* 2011; 93: 151–157.
11. Sharma A, Kumar Arya D, Dua M, et al. Nano-technology for targeted drug delivery to combat antibiotic resistance. *Expert Opin Drug Deliv* 2012; 9: 1325–1332.
12. Goldberg M, Langer R and Jia X. Nanostructured materials for applications in drug delivery and tissue engineering. *J Biomater Sci Polym Ed* 2007; 18: 241–268.
13. Hetrick EM and Schoenfisch MH. Reducing implant-related infections: active release strategies. *Chem Soc Rev* 2006; 35: 780–789.
14. Anderson EM, Noble ML, Garty S, et al. Sustained release of antibiotic from poly(2-hydroxyethyl methacrylate) to prevent blinding infections after cataract surgery. *Biomaterials* 2009; 30: 5675–5681.
15. Al-Kassas RS and El-Khatib MM. Ophthalmic controlled release in situ gelling systems for ciprofloxacin based on polymeric carriers. *Drug Deliv* 2009; 16: 145–152.

16. Kong M, Chen XG, Xing K, et al. Antimicrobial properties of chitosan and mode of action: a state of the art review. *Int J Food Microbiol* 2010; 144: 51–63.
17. Hanssen AD. Local antibiotic delivery vehicles in the treatment of musculoskeletal infection. *Clin Orthop Relat Res* 2005; 437: 91–96.
18. Brunet L, Lyon DY, Hotze EM, et al. Comparative photoactivity and antibacterial properties of C60 fullerenes and titanium dioxide nanoparticles. *Environ Sci Technol* 2009; 43: 4355–4360.
19. Hetrick EM, Shin JH, Stasko NA, et al. Bactericidal efficacy of nitric oxide-releasing silica nanoparticles. *ACS Nano* 2008; 2: 235–246.
20. Shen S-C, Ng WK, Shi Z, et al. Mesoporous silica nanoparticle-functionalized poly(methyl methacrylate)-based bone cement for effective antibiotics delivery. *J Mater Sci Mater Med* 2011; 22: 2283–2292.
21. Popat KC, Eltgroth M, LaTempa TJ, et al. Decreased Staphylococcus epidermis adhesion and increased osteoblast functionality on antibiotic-loaded titania nanotubes. *Biomaterials* 2007; 28: 4880–4888.
22. Vale N, Mäkilä E, Salonen J, et al. New times, new trends for ethionamide: in vitro evaluation of drug-loaded thermally carbonized porous silicon microparticles. *Eur J Pharm Biopharm* 2012; 81: 314–323.
23. Perelman LA, Pacholski C, Li YY, et al. pH-triggered release of vancomycin from protein-capped porous silicon films. *Nanomedicine (Lond)* 2008; 3: 31–43.
24. Gao P, Nie X, Zou M, et al. Recent advances in materials for extended-release antibiotic delivery system. *J Antibiot* 2011; 64: 625–634.
25. Kaur IP and Singh H. Nanostructured drug delivery for better management of tuberculosis. *J Control Release* 2014; 184: 36–50.
26. Yang C, Plackett D, Needham D, et al. PLGA and PHBV microsphere formulations and solid-state characterization: possible implications for local delivery of fusidic acid for the treatment and prevention of orthopaedic infections. *Pharm Res* 2009; 26: 1644–1656.
27. Yoon SJ, Kim SH, Ha HJ, et al. Reduction of inflammatory reaction of poly(D,L-lactic-co-glycolic acid) using demineralized bone particles. *Tissue Eng Part A* 2008; 14: 539–547.
28. Savage DJ, Liu X, Curley SA, et al. Porous silicon advances in drug delivery and immunotherapy. *Curr Opin Pharmacol* 2013; 13: 834–841.
29. Fine D, Grattoni A, Goodall R, et al. Silicon micro- and nanofabrication for medicine. *Adv Healthc Mater* 2013; 2: 632–666.
30. Salonen J, Kaukonen AM, Hirvonen J, et al. Mesoporous silicon in drug delivery applications. *J Pharm Sci* 2008; 97: 632–653.
31. Sakamoto JH, van de Ven AL, Godin B, et al. Enabling individualized therapy through nanotechnology. *Pharmacol Res* 2010; 62: 57–89.
32. Anglin EJ, Cheng L, Freeman WR, et al. Porous silicon in drug delivery devices and materials. *Adv Drug Deliv Rev* 2008; 60: 1266–1277.
33. McInnes SJ and Voelcker NH. Silicon-polymer hybrid materials for drug delivery. *Future Med Chem* 2009; 1: 1051–1074.
34. Godin B, Gu J, Serda RE, et al. Tailoring the degradation kinetics of mesoporous silicon structures through PEGylation. *J Biomed Mater Res A* 2010; 94: 1236–1243.
35. Limnell T, Riikonen J, Salonen J, et al. Surface chemistry and pore size affect carrier properties of mesoporous silicon microparticles. *Int J Pharm* 2007; 343: 141–147.
36. Prestidge CA, Barnes TJ, Lau C-H, et al. Mesoporous silicon: a platform for the delivery of therapeutics. *Expert Opin Drug Deliv* 2007; 4: 101–110.
37. Chiappini C, Tasciotti E, Fakhoury JR, et al. Tailored porous silicon microparticles: fabrication and properties. *Chemphyschem* 2010; 11: 1029–1035.
38. Murphy MB, Khaled SM, Fan D, et al. A multifunctional nanostructured platform for localized sustained release of analgesics and antibiotics. *Eur J Pain Suppl* 2011; 5: 423–432.
39. Santos HA, Riikonen J, Salonen J, et al. In vitro cytotoxicity of porous silicon microparticles: effect of the particle concentration, surface chemistry and size. *Acta Biomater* 2010; 6: 2721–2731.
40. Bimbo LM, Sarparanta M, Santos HA, et al. Biocompatibility of thermally hydrocarbonized porous silicon nanoparticles and their biodistribution in rats. *ACS Nano* 2010; 4: 3023–3032.
41. Salonen J, Laitinen L, Kaukonen A, et al. Mesoporous silicon microparticles for oral drug delivery: loading and release of five model drugs. *J Control Release* 2005; 108: 362–374.
42. Serda RE, Gu J, Bhavane RC, et al. The association of silicon microparticles with endothelial cells in drug delivery to the vasculature. *Biomaterials* 2009; 30: 2440–2448.
43. Tanaka T, Mangala LS, Vivas-Mejia PE, et al. Sustained small interfering RNA delivery by mesoporous silicon particles. *Cancer Res* 2010; 70: 3687–3696.
44. Tasciotti E, Liu X, Bhavane R, et al. Mesoporous silicon particles as a multistage delivery system for imaging and therapeutic applications. *Nat Nano* 2008; 3: 151–157.
45. Chhablani J, Nieto A, Hou H, et al. Oxidized porous silicon particles covalently grafted with daunorubicin as a sustained intraocular drug delivery system. *Invest Ophthalmol Vis Sci* 2013; 54: 1268–1279.
46. Liu D, Bimbo LM, Mäkilä E, et al. Co-delivery of a hydrophobic small molecule and a hydrophilic peptide by porous silicon nanoparticles. *J Control Release* 2013; 170: 268–278.
47. Wang M, Coffer JL, Dorraj K, et al. Sustained antibacterial activity from triclosan-loaded nanostructured mesoporous silicon. *Mol Pharm* 2010; 7: 2232–2239.
48. Santos HA, Bimbo LM, Lehto VP, et al. Multifunctional porous silicon for therapeutic drug delivery and imaging. *Curr Drug Discov Technol* 2011; 8: 228–249.
49. Furuya EY and Lowy FD. Antimicrobial-resistant bacteria in the community setting. *Nat Rev Microbiol* 2006; 4: 36–45.
50. Prokuski L. Prophylactic antibiotics in orthopaedic surgery. *J Am Acad Orthop Surg* 2008; 16: 283–293.
51. Patel R. Biofilms and antimicrobial resistance. *Clin Orthop Relat Res* 2005; 437: 41–47.
52. Low SP, Williams KA, Canham LT, et al. Generation of reactive oxygen species from porous silicon microparticles

in cell culture medium. *J Biomed Mater Res A* 2010; 93: 1124–1131.
53. Cohen MH, Melnik K, Boiarski AA, et al. Microfabrication of silicon-based nanoporous particulates for medical applications. *Biomed Microdevices* 2003; 5: 253–259.
54. Salonen J and Lehto VP. Fabrication and chemical surface modification of mesoporous silicon for biomedical applications. *Chem Eng J* 2008; 137: 162–172.
55. Serda RE, Ferrati S, Godin B, et al. Mitotic trafficking of silicon microparticles. *Nanoscale* 2009; 1: 250–259.
56. Liang D, Chow D and White C. High-performance liquid chromatographic assay of cefazolin in rat tissues. *J Chromatogr B Biomed Sci Appl* 1994; 656: 460–465.
57. Murphy MB, Blashki D, Buchanan RM, et al. Adult and umbilical cord blood-derived platelet-rich plasma for mesenchymal stem cell proliferation, chemotaxis, and cryopreservation. *Biomaterials* 2012; 33: 5308–5316.
58. Kilpeläinen M, Mönkäre J, Vlasova MA, et al. Nanostructured porous silicon microparticles enable sustained peptide (Melanotan II) delivery. *Eur J Pharm Biopharm* 2011; 77: 20–25.
59. Hughes GA. Nanostructure-mediated drug delivery. *Nanomedicine* 2005; 1: 22–30.
60. Olson ME and Horswill AR. *Staphylococcus aureus* osteomyelitis: bad to the bone. *Cell Host Microbe* 2013; 13: 629–631.
61. Wikler MA. *Performance standards for antimicrobial susceptibility testing: sixteenth informational supplement. Clinical and Laboratory Standards Institute*, http://isoforlab.com/phocadownload/csli/M100-S16.pdf (2006).
62. Martinez JO, Boada C, Yazdi IK, et al. Short and long term, in vitro and in vivo correlations of cellular and tissue responses to mesoporous silicon nanovectors. *Small* 2013; 9: 1722–1733.
63. Martinez JO, Evangelopoulos M, Chiappini C, et al. Degradation and biocompatibility of multistage nanovectors in physiological systems. *J Biomed Mater Res A*. Epub ahead of print 16 November 2013. DOI:10.1002/jbm.a.35017.
64. Tanaka T, Godin B, Bhavane R, et al. In vivo evaluation of safety of nanoporous silicon carriers following single and multiple dose intravenous administrations in mice. *Int J Pharm* 2010; 402: 190–197.
65. Low SP, Voelcker NH, Canham LT, et al. The biocompatibility of porous silicon in tissues of the eye. *Biomaterials* 2009; 30: 2873–2880.
66. Balmayor ER, Azevedo HS and Reis RL. Controlled delivery systems: from pharmaceuticals to cells and genes. *Pharm Res* 2011; 28: 1241–1258.
67. Huh AJ and Kwon YJ. "Nanoantibiotics": a new paradigm for treating infectious diseases using nanomaterials in the antibiotics resistant era. *J Control Release* 2011; 156: 128–145.
68. Wu P and Grainger DW. Drug/device combinations for local drug therapies and infection prophylaxis. *Biomaterials* 2006; 27: 2450–2467.
69. Engler AC, Wiradharma N, Ong ZY, et al. Emerging trends in macromolecular antimicrobials to fight multi-drug-resistant infections. *Nano Today* 2012; 7: 201–222.
70. Pelgrift RY and Friedman AJ. Nanotechnology as a therapeutic tool to combat microbial resistance. *Adv Drug Deliv Rev* 2013; 65: 1803–1815.
71. Hajipour MJ, Fromm KM, Akbar Ashkarran A, et al. Antibacterial properties of nanoparticles. *Trends Biotechnol* 2012; 30: 499–511.
72. De Rosa E, Chiappini C, Fan D, et al. Agarose surface coating influences intracellular accumulation and enhances payload stability of a nano-delivery system. *Pharm Res* 2011; 28: 1520–1530.
73. Murphy MB, Blashki D, Buchanan RM, et al. Multicomposite bioactive osteogenic sponges featuring mesenchymal stem cells, platelet-rich plasma, nanoporous silicon enclosures, and peptide amphiphiles for rapid bone regeneration. *J Funct Biomater* 2011; 2: 39–66.
74. Fan D, De Rosa E, Murphy MB, et al. Mesoporous silicon-PLGA composite microspheres for the double controlled release of biomolecules for orthopedic tissue engineering. *Adv Funct Mater* 2012; 22: 282–293.
75. Parodi A, Quattrocchi N, van de Ven AL, et al. Synthetic nanoparticles functionalized with biomimetic leukocyte membranes possess cell-like functions. *Nat Nano* 2013; 8: 61–68.